Nature of the Coupling between the High-Spin Fe(III) Heme and Cu_B(II) in the Active Site of Terminal Oxidases: Dual-Mode EPR Spectra of Fluoride Cytochrome *bo*$_3$

Vasily S. Oganesyan,[‡] Clive S. Butler,[‡,§] Nicholas J. Watmough,[§] Colin Greenwood,[§] Andrew J. Thomson,[‡] and Myles R. Cheesman*[,‡]

Centre for Metalloprotein Spectroscopy and Biology School of Chemical Sciences School of Biological Sciences University of East Anglia, Norwich NR4 7TJ, U.K.

Received December 1, 1997

Bacterial quinol oxidase (QO), known as cytochrome bo_3 (bo_3) and cytochrome *c* oxidase (CCO) reduce oxygen to water at a dinuclear heme−Cu site.[1,2] Crystal structures of oxidized CCO from *Paracoccus denitrificans*[3] and from bovine heart mitochondria[4,5] show the dinuclear site to have an Fe(III) heme, ligated by a proximal histidine, facing a copper ion (Cu_B) bound to three histidines. Although the Fe(III)−Cu(II) distance is estimated to be 4.5−5.0 Å the identity of the electron density, and hence, the nature of ligands bound between the metal ions remains unclear. Sequence comparisons and spectroscopic evidence establish a close structural homology of CCO and QO.[6] In the oxidized QO, a variety of ligands including F^-, $HCOO^-$, and H_2O will bind the heme which remains high-spin Fe(III), $S = {}^5/_2$, whereas N_3^- binds to Cu_B(II).[7,8] Perpendicular-mode X-band EPR spectra of all these derivatives show broad, fast relaxing features with a similar pattern of bands: a weak derivative signal below 100 mT ($g \approx 12$ region) accompanied by a broad band in the region 200−250 mT ($g \approx 3.2$).[9] In the parallel-mode spectrum, only the low-field signal is present. Similar signals have been reported for the *slow* form of CCO.[10,11] Much experimental and theoretical effort has been expended in order to obtain an energy level scheme which will account for these EPR spectra and for the magnetic properties of the dinuclear center in CCO, primarily with a view to arriving at an estimate of the magnitude, and sign, of the exchange coupling between the high-spin heme and the Cu_B. Invariably these models have concluded that the metals are *strongly coupled* with $|\boldsymbol{J}| > 10^2$ cm^{-1}. We present here the first successful simulation of both perpendicular- and parallel-mode X-band EPR spectra of fluoride bo_3 (prepared at pH 7.4 as previously described[7,9]). This shows only a very weak ($|\boldsymbol{J}| \approx 1$ cm^{-1}) exchange interaction between the two ions and poses intriguing questions about the pathway of coupling. It also suggests that intervening exogenous ligands play a minor part in mediating this interaction.

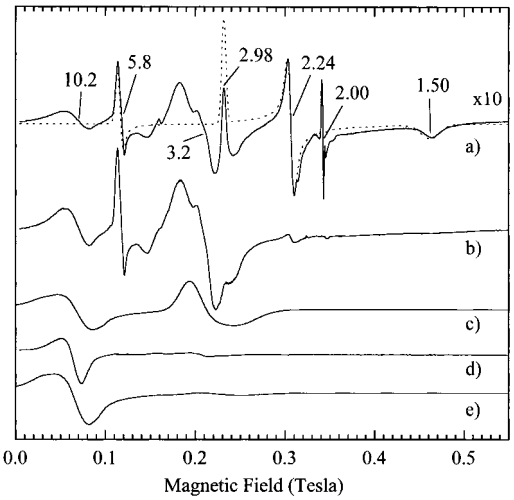

Figure 1. X-band EPR spectra of fluoride bo_3: (a) perpendicular-mode spectrum at 10 K and 2.03 mW; (b) perpendicular-mode spectrum at 5 K and 103 mW; (c) simulation of b; (d) parallel-mode spectrum at 5 K and 103 mW; (e) simulation of d. The simulations shown were achieved using the following parameters: $D = 5.0$ cm^{-1}; $E = 0.3$ cm^{-1}; $J_{xyz} = -0.337, -0.337, -2.300$ cm^{-1}, isotropic line widths of 0.004 cm^{-1} ($g = 10.2$ feature) and 0.01 cm^{-1} ($g = 3.2$ feature) and a Gaussian distribution in E with a line width of 0.031 cm^{-1}.

The perpendicular-mode X-band EPR spectrum of fluoride bo_3, at 10 K with low microwave power (2.03 mW) (Figure 1a), shows low-spin Fe(III) heme *b* signals at $g = 2.98$, 2.24, and 1.50 and a sharp derivative at $g = 5.8$ from ∼4% high-spin Fe(III) heme o_3 uncoupled from Cu_B(II).[14] At 5 K with 103 mW power, broad derivative-shaped features near $g = 10.2$ and 3.2 dominate the spectrum (Figure 1b). They arise from the dinuclear site.[9] The heme *b* features are saturated under these conditions and are almost undetectable. The parallel-mode spectrum (5 K and 103 mW) (Figure 1d) contains an intense derivative-shaped band at 70 mT but only very weak intensity near $g = 3.2$. Signals due to heme *b* and decoupled heme o_3 are absent from the parallel-mode spectrum as expected for $\Delta M_S = \pm 1$ transitions within Kramers doublets.[15,16] Experimental intensities have been adjusted to allow for spectrometer gain. The $S = {}^1/_2$ spectrum of heme *b* serves as an internal standard, and its simulation was used to normalize simulations of the broad features. This allows direct comparison of spectrum intensities as presented. Spectra c and e Figure 1 are simulations of the perpendicular- and parallel-mode EPR features from the dinuclear site. These are based on a theoretical model in which the energy levels of two interacting metal ions can be described by the spin Hamiltonian:[15]

$$\hat{\boldsymbol{H}} = [g\beta B\hat{S} + D(\hat{S}_z^{\,2} - \hat{S}^2/3) + E(\hat{S}_x^{\,2} - \hat{S}_y^{\,2})]^{Fe} + [g\beta B\hat{S}]^{Cu} - \hat{S}_{Fe}\cdot\boldsymbol{J}\cdot\hat{S}_{Cu} \quad (1)$$

The first term represents the Zeeman interaction and zero-field

* Address correspondence to this author at the School of Chemical Sciences, University of East Anglia, Norwich, NR4 7TJ, United Kingdom. Telephone: +44 (1603) 592028. Facsimile: +44 (1603) 592710. E-mail: m.cheesman@uea.ac.uk.

‡ School of Chemical Sciences.

§ School of Biological Sciences.

(1) Trumpower, B. L.; Gennis, R. B. *Annu. Rev. Biochem.* **1994**, *63*, 675−716.

(2) Watmough, N. J.; Cheesman, M. R.; Butler, C. S.; Little, R. H.; Greenwood, C.; Thomson, A. J. *J. Bioenerg. Biomemb.* **1998**, *30*, 55−62.

(3) Iwata, S.; Ostermeier, C.; Ludwig, B.; Michel, H. *Nature* **1995**, *376*, 660−669.

(4) Tsukihara, T.; Aoyama, H.; Yamashita, E.; Tomizaki, T.; Yamaguchi, H.; Shinzawa-Itoh, K.; Nakashima, R.; Yaono, R.; Yoshikawa, S. *Science* **1995**, *269*, 1069−1074.

(5) Tsukihara, T.; Aoyama, H.; Yamashita, E.; Tomizaki, T.; Yamaguchi, H.; Shinzawa-Itoh, K.; Nakashima, R.; Yaono, R.; Yoshikawa, S. *Science* **1996**, *272*, 1136−1144.

(6) Chepuri, V.; Lemieux, L.; Au, D. C.-T.; Gennis, R. B. *J. Biol. Chem.* **1990**, *265*, 11185−11192.

(7) Cheesman, M. R.; Watmough, N. J.; Gennis, R. B.; Greenwood, C.; Thomson, A. J. *Eur. J. Biochem.* **1993**, *219*, 595−602.

(8) Little, R. H.; Cheesman, M. R.; Thomson, A. J.; Greenwood, C.; Watmough, N. J. *Biochemistry* **1996**, *35*, 13780−13787.

(9) Watmough, N. J.; Cheesman, M. R.; Gennis, R. B.; Greenwood, C.; Thomson, A. J. *FEBS Lett.* **1993**, *319*, 151−154.

(10) Greenaway, F. T.; Chan, S. H. P.; Vincow, G. *Biochim. Biophys. Acta* **1977**, *490*, 62−68.

(11) Hagen, W. R. *Biochim. Biophys. Acta* **1982**, *708*, 82−98.

(12) Moss, T. H.; Shapiro, E.; King, T. E.; Beinert, H.; Hartzell, C. *J. Biol. Chem.* **1978**, *253*, 8072−8073.

(13) Dunham, W. R.; Sands, R. H.; Shaw, R. W.; Beinert, H. *Biochim. Biophys. Acta* **1983**, *748*, 73−85.

(14) Cheesman, M. R.; Watmough, N. J.; Pires, C. A.; Turner, R.; Brittain, T.; Gennis, R. B.; Greenwood, C.; Thomson, A. J. *Biochem. J.* **1993**, *289*, 709−718.

(15) Hendrich, M. P.; Münck, E.; Fox, B. G.; Lipscomb, J. D. *J. Am. Chem. Soc.* **1990**, *112*, 5861−5865.

(16) Hendrich, M. P.; Debrunner, P. G. *Biophys. J.* **1989**, *56*, 489−506.

S0002-7863(97)04050-X CCC: $15.00
Published on Web 04/17/1998

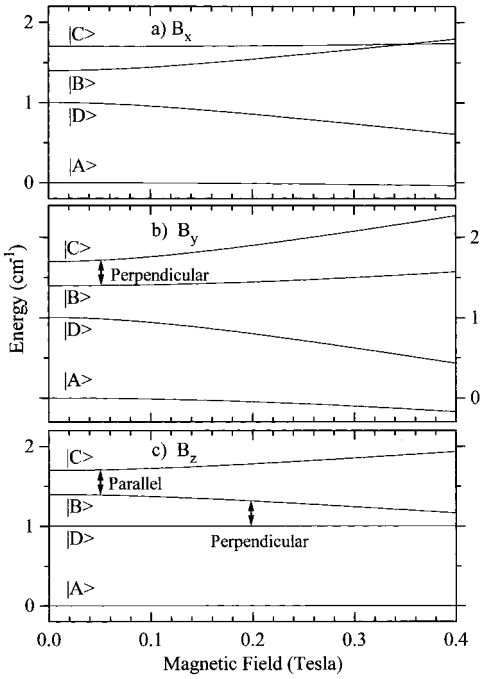

Figure 2. Energies of the four states formed by exchange coupling of effective spins, $S = {}^1/_2$, on high-spin Fe(III) heme and Cu_B(II) as described in text with magnetic field along the three principal molecular axes.

splittings (ZFS) at iron (*D* and *E* are the axial and rhombic ZFS parameters), the second represents the Zeeman interaction at Cu_B(II), and the third represents the spin coupling between the two metals defined by ***J***, the exchange coupling tensor. A basis set is constructed using products of the single ion spin functions $|S_1,M_1\rangle|S_2,M_2\rangle$, where S_1 and S_2 refer to the total spins of the individual ions. For high-spin Fe(III) and Cu(II), $S_1 = {}^5/_2$ and $S_2 = {}^1/_2$. In the limit of *strong exchange coupling*, $|\boldsymbol{J}| \gg |D|$, the twelve product functions split into two multiplets of total spin $S' = 2$ and $S' = 3$. For $|\boldsymbol{J}| \ll |D|$, the *weak coupling limit*, using a *D*-value at Fe(III) heme of 5.0 cm^{-1}, the $S = {}^5/_2$ levels of Fe(III) are split into three Kramers pairs, with effective spin $S = {}^1/_2$ lying 10 cm^{-1} (2*D*) below the next pair. An isotropic *J* of ~1 cm^{-1} couples this pair with the $S = {}^1/_2$ Kramers pair from Cu_B(II) to give four energy states (eq 2). In order of ascending energy the effective spin components along the Fe−Cu axis are 0, +1, −1, 0.

$$|A\rangle = \frac{1}{\sqrt{2}}\left(\left|\frac{1}{2},\frac{-1}{2}\right\rangle - \left|\frac{-1}{2},\frac{1}{2}\right|\right) \qquad M_S = 0$$

$$|B\rangle = -\sin\phi\,|\frac{3}{2},\frac{-1}{2}\rangle + \cos\phi\,|\frac{1}{2},\frac{1}{2}\rangle \qquad M_S = +1$$

$$|C\rangle = -\sin\phi\,|\frac{-3}{2},\frac{1}{2}\rangle + \cos\phi\,|\frac{-1}{2},\frac{-1}{2}\rangle \qquad M_S = -1$$

$$|D\rangle = \frac{1}{\sqrt{2}}\left(\left|\frac{1}{2},\frac{-1}{2}\right\rangle + \left|\frac{-1}{2},\frac{1}{2}\right|\right) \qquad M_S = 0 \quad (2)$$

where $\tan 2\phi = \sqrt{8}J/(2D - J)$. $|B\rangle$ and $|C\rangle$ are axially degenerate except in the presence of a rhombic distortion, *E*. Anisotropy of the ***J***-tensor (eq 1) is required to account satisfactorily both for the observed resonant field values and the relative transition intensities in parallel and perpendicular modes. The resulting energy levels as a function of $B_{x,y,z}$, the magnetic field along each principal axis, are given in Figure 2. Simulated spectra (Figure 1) have been averaged over all orientations of field with respect to the molecular frame and over *E* assuming a Gaussian distribution of rhombicity.[16]

The low-field signal, $g \approx 10.2$, formally $\Delta M_S = \pm 2$, is due to a transition between levels $|B\rangle$ and $|C\rangle$. With a magnetic field parallel to *Z*, the heme perpendicular, parallel-mode intensity is allowed but perpendicular-mode forbidden.[17] When the field is directed along the *Y* axis (Figure 2), the Zeeman interaction mixes $|A\rangle$ with $|B\rangle$ and $|C\rangle$ with $|D\rangle$ separating the two states to satisfy the resonance condition at approximately the same resonance field and with essentially the same transition intensity as in parallel mode. Thus, the model correctly accounts for both the intensity ratio (~1/1.3) and the shifts in positions of the signals between the two modes.

The $g = 3.2$ signal arises from a transition between levels $|D\rangle$ and $|B\rangle$ and, hence, is formally $\Delta M_S = \pm 1$. Therefore, this transition has intensity predominantly in the perpendicular mode. However, the Zeeman interaction is highly anisotropic. With fields along *X* and *Y*, the energy level separation at zero-field is greater than the energy of an X-band photon, and thus, these two orientations make no significant contribution to the EPR intensity. This occurs primarily when the magnetic field is along *Z*.

Previous work has assigned the transition at $g = 12$ in CCO to a $\Delta M_{S'} = \pm 4$ transition within an $M_{S'} = \pm 2$ non-Kramers pair of an $S' = 2$ system using a D'-value of 1.19 cm^{-1} in a Hamiltonian that assumes the *strong coupling* limit.[11] The relationship between *D*, the axial ZFS parameter of high spin Fe(III) heme, and D' is $D' \approx (4/3)D$.[18] Hence, the value of 0.9 cm^{-1} obtained for *D* is too small for a high-spin Fe(III) heme with proximal histidine ligation which is more typically 5−8 cm^{-1}.[19] Theoretical models based on the strong coupling limit have also been used to interpret data from Mössbauer and susceptibility measurements, but none has satisfactorily addressed the problem of the anomalously small value of *D*.[11−13,20−22] No previous attempts have been made to assign the transition at $g \approx 3.2$, although the present work shows that this severely restrains the coupling model. Attempts to simulate both parallel and perpendicular mode EPR features at $g = 10.2$ and 3.2 within a strong coupling model have proved unsuccessful.

The theoretical model presented represents a significant improvement in our understanding of the interaction between high-spin Fe(III) heme and copper(II) ion at the active site of heme−copper oxidases. The results show clearly that the two metal ions are coupled only weakly with $|\boldsymbol{J}|$ values of the order of 1 cm^{-1} when fluoride ion is the ligand to heme. Similar results have been obtained for the *fast*, formate, and azide derivatives of bo_3.[23] This shows that the interaction is weak in origin and not greatly influenced by any ligand between the two metal ions provided that the heme remains high spin. This contrasts with the situation when cyanide ion is bound at the dinuclear center.[24] In this case, the ligand switches the heme low spin and couples the two spins ferromagnetically by bridging both metal ions.

Acknowledgment. We are grateful to R.B. Gennis for supplying strains of *Escherichia coli*. The CMSB is supported by a rolling grant from EPSRC/BBSRC. V.S.O. and C.S.B are supported by BBSRC grants and N.J.W. by Wellcome Trust Career Development Fellowship.

JA974050O

(17) Abragam, A.; Bleaney, B. *Electron Paramagnetic Resonance of Transition Ions;* Clarendon Press: Oxford, 1970.
(18) Buluggiu, E. *J. Phys. Chem. Solids* **1980**, *41*, 43−45.
(19) Brudvig, G. W.; Stevens, T. H.; Morse, R. H.; Chan, S. I. *Biochemistry* **1981**, *20*, 3912−3921.
(20) Kent, T. A.; Young, L. J.; Palmer, G.; Fee, J. A.; Münck, E. *J. Biol. Chem.* **1983**, *258*, 8543−8546.
(21) Barnes, Z. K.; Babcock, G. T.; Dye, J. L. *Biochemistry* **1991**, *30*, 7597−7603.
(22) Day, E. D.; Peterson, J.; Sendova, M. S.; Schoonover, J. R.; Palmer, G. *Biochemistry* **1993**, *32*, 7855−7860.
(23) The analysis of variable temperature/magnetic field MCD data on fluoride bo_3 has now been completed and provides independent evidence for the weak-coupling scheme.
(24) Thomson, A. J.; Eglinton, D. G.; Hill, B. C.; Greenwood, C. *Biochem. J.* **1982**, *207*, 167−170.